ORIGINAL PAPER

Determining symmetry changes during a chemical reaction: the case of diazene isomerization

Inbal Tuvi-Arad · David Avnir

Abstract   Analysis of reaction paths in terms of the Continuous Symmetry Measure (CSM) provides an alternative way to analyze the geometrical changes that take place during a reaction. Unique symmetry-profiles, describing the symmetry changes along the internal reaction coordinate were calculated for the *cis-trans* isomerization reaction of N_2H_2 and for its halogeno derivatives. A "symmetry transition point" is identified at the extremum point along the symmetry-profiles. At this point, the deviation of the molecule from the rotational symmetry of the reactant is the same as its deviation from the rotational symmetry of the product. In a second application we show that the CSM can be used as an alternative reaction coordinate. Calculations at the MP2 and DFT levels result in similar symmetry profiles.

1 Introduction

Specific geometrical changes which take place in the course of a chemical reaction are traditionally described in terms of variations in bond lengths, bond angles and dihedral angles. Since in the course of a reaction usually all of these specific parameters change simultaneously, the structural follow-up of a reaction can be quite complex. Simplification in the form of a global structural parameter which unifies these spe-

I. Tuvi-Arad
Department of Natural Sciences, The Open University of Israel, 43107 Raanana, Israel

D. Avnir (✉)
Institute of Chemistry and The Lise Meitner Minerva Center for Computational Quantum Chemistry,
The Hebrew University of Jerusalem, 91904 Jerusalem, Israel
e-mail: david@chem.ch.huji.ac.il

cific parameters into a single descriptor is therefore an interesting alternative to this approach. In this paper we present a preliminary exploration of this kind by describing reaction paths in terms of a unique symmetry measure.

Symmetry is an important factor in determining the interaction between molecules; the frontier orbital theory of Fukui [1,2] and the Woodward and Hoffman rules [3,4], are celebrated examples. Thus, a quantitative way to describe the symmetry changes during a reaction is desirable. In the last two decades, several symmetry and similarity measures have been developed, e.g., the pioneering work of Mezey et al. [5–7] on chemical similarity measures and quantum molecular similarity measures in the context of electron density analysis [8] and shape analysis. In particular, Mezey developed general rules that describe the rate of convergence of symmetry deficiency measures along chemical reaction paths [9–11]. Similarity measures have also been used in QSAR studies [12–14] and DNA sequence analysis [15]. Here we focus on the continuous symmetry measure (CSM) [16–20], which is a global structural parameter, and which provides a quantitative estimate of the degree of molecular symmetry. This measure is particularly useful for comparing the symmetry of different molecules, or symmetry changes within a molecule. The CSM approach, as do other symmetry and similarity measures, expands the binary language of symmetry: Rather than defining a particular molecule as symmetric or not, one can—by the CSM approach—determine its content-level with respect to any desirable symmetry on a continuous scale. This measure represents, by a single number, the collection of geometrical parameters that defines the original structure. Since its original development, the method has been broadened to measure chirality [21,22] and shape [23–26] and proven to be useful for describing correlations between these structural features and a host of physical, chemical, and biochemical observables. Recent examples include the shape of inorganic complexes [27–29,31], chirality measures in QSAR [32,33] and chirality of both organic [34,35] and inorganic [36] compounds. Several applications of the CSM to study chemical reactions have been published in the last decade. Examples are the work by Llunell et al. who studied the mechanism of narcissistic reactions [37]; the works of Pinto et al. on the Stone-Wales rearrangements in fullerenes [38] and the classification of enantiomerization pathways of butane-like molecules [39]; and the work of Alemany et al. on the racemization reaction of hexacoordinated transition-metal complexes [40].

In this article, we report on an application of the CSM approach to the study of reaction paths as represented by the intrinsic reaction coordinate (IRC) method [41–45]. For this purpose, we chose the cis-trans isomerization reaction of diazene (N_2H_2) and of its halogeno derivatives, which have been intensively studied [46–57]. Azo compounds, of the form RN=NR, undergo a reversible cis-trans isomerization either thermally or photochemically, which makes them potential candidates for molecular switches or for optical data storage systems [52,53,58–60]. Diazene, the simplest form of these compounds, is also interesting because of its ability to stereospecifically reduce olefinic bonds [61]. Several mechanisms have been suggested for the *cis-trans* isomerization of diazene: inversion, rotation about the N=N double bond, and cleavage followed by a subsequent recombination. As shown by Sokalski et al. [53], the inversion mechanism is the preferable one for the *cis-trans* isomerization of neutral diazene. Therefore, we focused on this mechanism, which is described below.

Continuous symmetry analysis of the systems studied here uncovers interesting data about the structural changes that the reactant undergoes during the reaction. We also show that the CSM can be used as an alternative reaction coordinate.

2 Computational methods

2.1 IRC calculations

These were performed using Gaussian03 [62] for N_2X_2 (X = H, F, Cl). Calculations were carried out at two different levels of theory: Møller-Plesset second-order perturbation theory (MP2) [63] and density functional theory (DFT) using the B3LYP [64,65,67] correlation functional. In both cases, the correlation consistent polarized valence double-zeta (CC-PVDZ) [68] basis set was used. These levels were chosen to provide reasonable accuracy. All IRC calculations were verified by repeating them with a smaller step size, and transition state (TS) geometries were compared to the literature wherever possible. We do not attempt to provide the most accurate calculations, rather to show trends and relations between two methods. As our results show, calculations of the CSM are almost unaffected by the choice of the model.
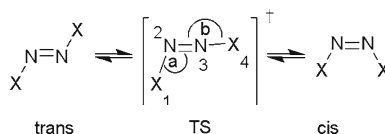
2.2 CSM calculations

These calculations are based on finding the minimal distance between a given structure and the nearest, searched structure that belongs to the desired symmetry point group [16–18,20,69]. For a structure composed of N vertices, the coordinates of which are $\{\mathbf{Q}_k, \quad k = 1, 2, \ldots N\}$, we calculate how much of G-symmetry it has, where G is a symmetry point group. Let the coordinates of the searched, nearest perfectly G-symmetric object be at $\{\mathbf{P}_k, \quad k = 1, 2, \ldots N\}$. The continuous symmetry measure is defined as:

$$S(G) = 100 \times \min \frac{\sum\limits_{k=1}^{N} |\mathbf{Q}_k - \mathbf{P}_k|^2}{\sum\limits_{k=1}^{N} |\mathbf{Q}_k - \mathbf{Q}_0|^2} \tag{1}$$

Here $\mathbf{Q}_0$ is the coordinate vector of the center of mass of the investigated structure. The denominator in Eq. (1) is a mean square size normalization factor which is introduced to avoid size effects. The CSM defined in Eq. (1) is a normalized root-mean-square deviation from the closest structure with the desired symmetry and is independent of the position, orientation, and size of the original structure. The bounds of $S(G)$ are between zero and 100. If a structure has the desired G-symmetry, then $S(G) = 0$ and the symmetry measure increases as it departs from G-symmetry. It is important to note that the structure with the desired symmetry is unknown at the beginning of the calculation. The algorithm is based on searching for structures with the desired symmetry, and then selecting the one that has the minimal distance from the original structure, according to Eq. (1).

Fig. 1 The inversion mechanism for the N_2X_2 *cis-trans* isomerization reaction. X = H, F, Cl

trans   TS   cis

Fig. 2 The symmetry elements used for the CSM calculations. **a** *trans*-N_2H_2—inversion point and a C_2 rotation axis, **b** *cis*-N_2H_2—reflection plane and a C_2 rotation axis

a *trans*   **b** *cis*
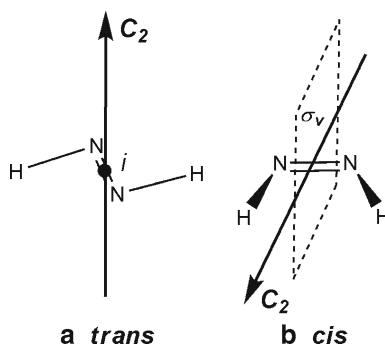
Applying Eq. (1) to molecules requires, as input, the coordinates of the studied structure, the connectivity of the atoms in the molecule (a list that specifies the way atoms are connected to each other) and the specific permutation that defines the required symmetry. The permutation is a list that specifies which atoms are replaced by a specific symmetry operation. This is important in cases where there is more than one symmetry element of the same kind (e.g., reflection planes for *cis* diazene).

2.3 Reaction path and the inversion mechanism

The inversion mechanism for the *cis-trans* isomerization of diazene and its halogeno derivatives is shown schematically in Fig. 1. According to this mechanism, one of the hydrogen (or halogen) atoms rotates in plane from its original location to an opposite location relative to the N=N bond. The transition state (TS) is a planar structure. To represent the transition from *cis* (C_{2v}) to *trans* (C_{2h}), several symmetry measures have been calculated, namely of C_2, C_s and C_i. Figure 2 represents the corresponding symmetry elements of *cis* and *trans* diazene. Note that the C_2 rotation axis is in plane for the *cis* isomer and perpendicular to the molecular plane for the *trans* isomer (Fig. 2). As for C_s, both *trans* and *cis* diazene have a reflection plane that coincides with the plane of the molecule, which is preserved throughout the isomerization (S = 0). Therefore we focused on the perpendicular plane, which characterizes the *cis* (the σ_v plane). Finally, C_i exists in the *trans* isomer but not in the *cis* isomer.

3 Results and discussion

3.1 The transition state

The general structure of N_2X_2 along the inversion mechanism is represented by the middle structure in Fig. 1. The geometrical parameters for the TS are summarized in

Table 1 Transition states of N_2X_2 (X = H, F, Cl)

	Geometric parameters[a]	B3LYP/ CCPVDZ	MP2/ CCPVDZ	MP2	QCISD/LANL2DZdp [54]	CASSCF/ 63111G(3df,2p) [53]
N_2H_2	α (deg)	109.6	108.8	109.2[b]	108.6	109.5
	β (deg)	177.3	177.6	178.0[b]	178.3	178.2
	R_{12} (Å)	1.079	1.068	1.062[b]	1.064	
	R_{23} (Å)	1.228	1.244	1.244[b]	1.251	1.237
	R_{34} (Å)	0.997	0.997	0.996[b]	1.007	
N_2F_2	α (deg)	110.2	109.6	108.9[c]		
	β (deg)	171.5	170.7	170.0[c]		
	R_{12} (Å)	1.642	1.711	1.743[c]		
	R_{23} (Å)	1.168	1.172	1.176[c]		
	R_{34} (Å)	1.301	1.296	1.303[c]		
N_2Cl_2	α (deg)	113.1	111.8			
	β (deg)	169.8	167.9			
	R_{12} (Å)	2.200	2.230			
	R_{23} (Å)	1.157	1.172			
	R_{34} (Å)	1.624	1.623			

[a] Parameters are defined in Fig. 1
[b] MP2/6-31G(d)b [49]
[c] MP2/DZP [46]

Table 1. As is evident from the table, there is good agreement between the B3LYP and MP2 results, and between our calculations and other methods reported in the literature: MP2/6-31G(d) [49] QCISD/LANL2DZdp [54], and CASSCF/6-3111G(3df,2p) [53] for diazene and MP2/DZP [46] for difluorodiazene. As will be shown, the minor differences between bond lengths and bond angles of the two methods are insignificant to the continuous symmetry analysis. Therefore, for the sake of simplicity, we will continue our discussion with the DFT calculations.

3.2 The IRC energy profile

Energy profiles calculated at the B3LYP/CC-PVDZ level along the IRC coordinate for the three N_2X_2 molecules are shown in Fig. 3. In order to present all curves on the same scale, the energies of each curve were scaled according to:

$$E_{rel} = E - E \text{ (reactant)} \tag{2}$$

DFT calculations on difluorodiazene lead to the *cis* isomer for negative IRC values and the *trans* isomer for positive IRC values. This is in contrast to diazene and dichlorodiazene for which negative IRC values lead to the *trans* isomer and positive IRC values resulted in the *cis* isomer. In order for all reactions paths to start with the *trans* isomer at negative IRC values, the IRC values for difluorodiazene were reversed (i.e.,

Fig. 3 Energy profiles for the
N₂X₂ *cis-trans* isomerization
reaction (X = H, F, Cl) calculated
at the B3LYP/CC-PVDZ level.
Energies have been scaled
according to Eq. (2)
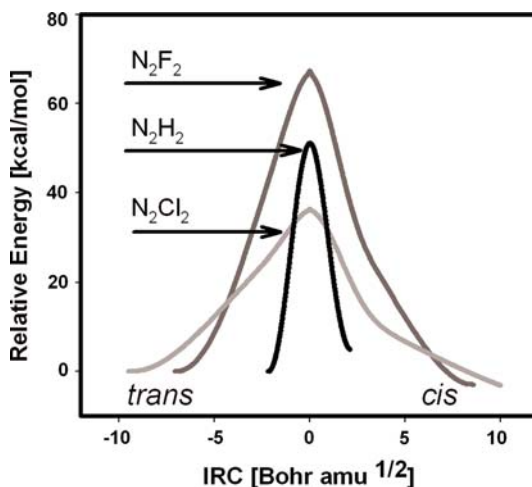
IRC → -IRC) in Fig. 3. As is evident from Fig. 3, the *trans* isomer is more stable for
diazene while the *cis* isomer is more stable for difluorodiazene and dichlorodiazene.
As has been reported before, the *cis* effect originates from the dominance of lone-pair
hyperconjugation on the basic electronic structure and energetic natures of 1,2-dihalo-
diazene systems [52,56]. Calculations at the MP2 level gave similar results and are
not shown here.

3.3 Symmetry changes along the IRC coordinate

The CSM can be used to describe reactions in two different ways. The first, as a newly
defined structural property that changes along the IRC, which we term the "symme-
try profile of the reaction." The second—as an alternative reaction coordinate—is
described in the next section. Figure 4 presents the symmetry profiles of the N₂X₂
cis-trans isomerization reaction with respect to the C_2 rotation group: each point along
the curve answers the question: How far is the structure from having C_2 symmetry?
Two main observations can be made:

a. The symmetry profile curves have a discontinuous maximum point. We call this
    point a **symmetry transition point** (STP): The structure at this point is the far-
    thest—along the reaction pathway (as represented by the IRC or by other coordi-
    nates)—from having the analyzed symmetry. In our example, the reason for the
    discontinuity is that left to the STP, the nearest symmetric structure at each point
    resembles the *trans* isomer, and the rotation axis is perpendicular to the molecular
    plane; to the right the nearest symmetric structure at each point resembles the *cis*
    isomer and the rotation axis is in plane (see Fig. 2). Also, in our case, the sym-
    metry deviation from the reactant symmetry equals its deviation from the product
    because both ends are of S = 0 values; in general this need not be the case. Note
    that the STP is different from the TS: The geometrical parameters of the STPs
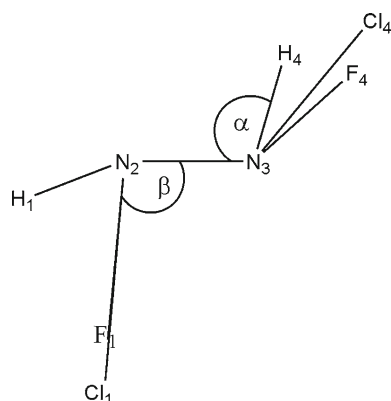   for the N₂X₂ reactions are presented in Table 2. Cases where the points coincide
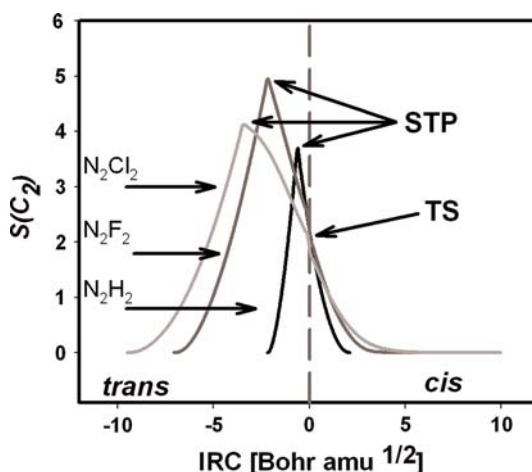
are possible and will be reported separately. As can be seen from Table 2, the geometry of the STPs calculated at the B3LYP level is in very good agreement with the MP2 calculation.

b. The value of $S(C_2)$ at the STP can be treated as a measure of the maximum distortion (in terms of rotational symmetry) that the molecule undergoes during the reaction along the IRC. It is highest for N_2F_2 and decreases in the order F > Cl > H. A similar trend was obtained at the MP2 level of calculation. In other words, the isomerization process of *cis*-N_2F_2 to *trans*-N_2F_2 undergoes more symmetry distortion as compared with N_2Cl_2 and N_2H_2. Figure 5 shows the STP structures of the different molecules superimposed on each other. The trend of the distortion may be related to the lone pair hyperconjugation effect as discussed by Yamamoto et al. [56], and requires further investigation.

In order for an STP to emerge, distortion from a symmetry element which exists (or nearly exists) in the reactant and product must characterize the reaction pathway. Other relevant symmetries need not follow this rule, and the distortion may grow continuously along the reaction coordinate. This is seen in Fig. 6 where, in addition to rotation, the behavior of inversion and reflection are shown. It is seen that their measures depart continuously from the isomers which are characterized by them (the *trans* isomer with inversion and the *cis* isomer with reflection symmetry (Fig. 2; the energy changes are also shown for reference). Having in mind the partial IRC calculations—which do not continue all the way to the reactant and product—and which are carried out to test the validity of a TS structure, plotting the deviation from symmetries that characterize a structure—reactant or product (inversion and reflection in this case) helps in identifying the reactant and product points, without need of their specific structures or of their energy difference. It is also seen that for the process *trans* → STP, $S(C_2) = S(C_i)$, while for the process STP → *cis*, $S(C_2) = S(C_s)$. In other words, for a *trans*-like structure—inversion and rotation lead to the same nearest symmetric structure, while for the *cis*-like structure, reflection and rotation lead to the same structure, as expected for two-dimensional molecules. Similar plots, not shown here, were obtained for N_2F_2 and N_2Cl_2.

Table 2 Symmetry transition points of N_2X_2 (X = H, F, Cl)

	Geometric parameters[a]	B3LYP/CC-PVDZ	MP2/CC-PVDZ
N_2H_2	α (deg)	106.7	105.7
	β (deg)	156.6	157.0
	R_{12} (Å)	1.066	1.067
	R_{23} (Å)	1.232	1.249
	R_{34} (Å)	1.006	1.007
	S (C_2)	3.6950	3.8010
	IRC (Bohr amu$^{1/2}$)	−0.59893	−0.59894
	Energy (kcal/mol)	−69,390.4	−69,192.8
N_2F_2	α (deg)	95.3	94.9
	β (deg)	139.4	139.6
	R_{12} (Å)	1.707	1.747
	R_{23} (Å)	1.184	1.191
	R_{34} (Å)	1.357	1.358
	S (C_2)	4.9376	5.0333
	IRC (Bohr amu$^{1/2}$)	−2.18819	−1.99975
	Energy (kcal/mol)	−193,877.5	−193,414.1
N_2Cl_2	α (deg)	94.5	94.3
	β (deg)	131.5	131.5
	R_{12} (Å)	2.241	2.248
	R_{23} (Å)	1.164	1.181
	R_{34} (Å)	1.797	1.781
	S (C_2)	4.1178	4.2420
	IRC (Bohr amu$^{1/2}$)	−3.38857	−3.14956
	Energy (kcal/mol)	−646,213.9	−645,277.8

[a] Parameters are defined in Fig. 5

Fig. 5 Geometry of the N_2X_2 molecules at the symmetry transition point (STP) superimposed one on the other. See Table 2 for bond lengths and bond angles
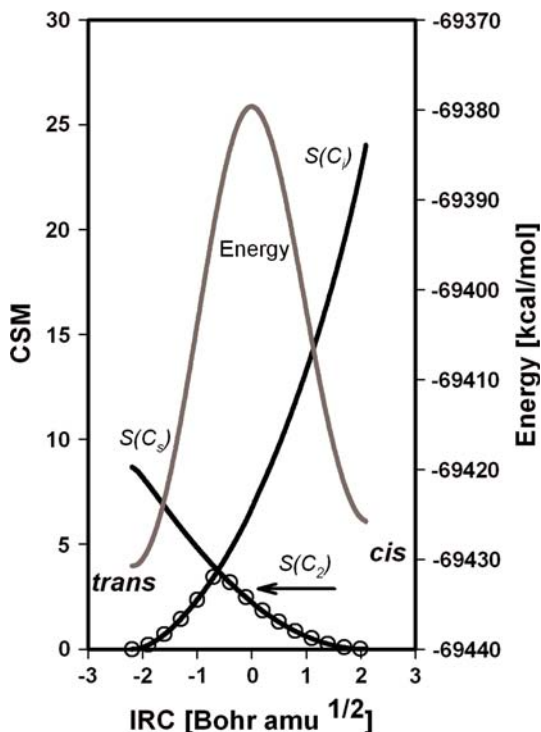
Figure 7 demonstrates, for the diazene system, the independence of the symmetry measures on the quantum-mechanical method—DFT or MP2—as compared to the sensitivity of the energy values: the symmetry profiles almost coincide. Calculations at the HF level, not shown here, gave less accurate results for the energy of the process, but similar results for the symmetry profiles. Similar results have been obtained for difluorodiazene and dichlorodiazene and are not shown here. Preliminary results on other systems imply that this effect is not particular to the N_2X_2 system. This behavior of the CSM as a structural parameter, suggests that a high level of IRC calculations may not be necessary for the symmetry analysis of reaction paths.

3.4 The symmetry measure as a reaction coordinate

The CSM can be used not only as a varying structural property, as demonstrated above, but also as a reaction coordinate, along which other process parameters—energy is the most common one—can be drawn. Figure 8 presents the energy profiles of the N_2X_2 *cis* → *trans* isomerization reactions (calculated at the B3LYP/CC-PVDZ level) using either $S(C_s)$ or $S(C_i)$ as reaction coordinates. Note that the reactant and product can be identified on these plots simply by their symmetry. The shape of these plots is similar to the regular energy profile with the transition state at the maximum point on each graph. Such shapes are obtained when the symmetry measure increases continu-

Fig. 7 Rotational symmetry profiles and energy profiles for the N_2H_2 *cis-trans* isomerization reaction: comparison of the DFT and MP2 methods
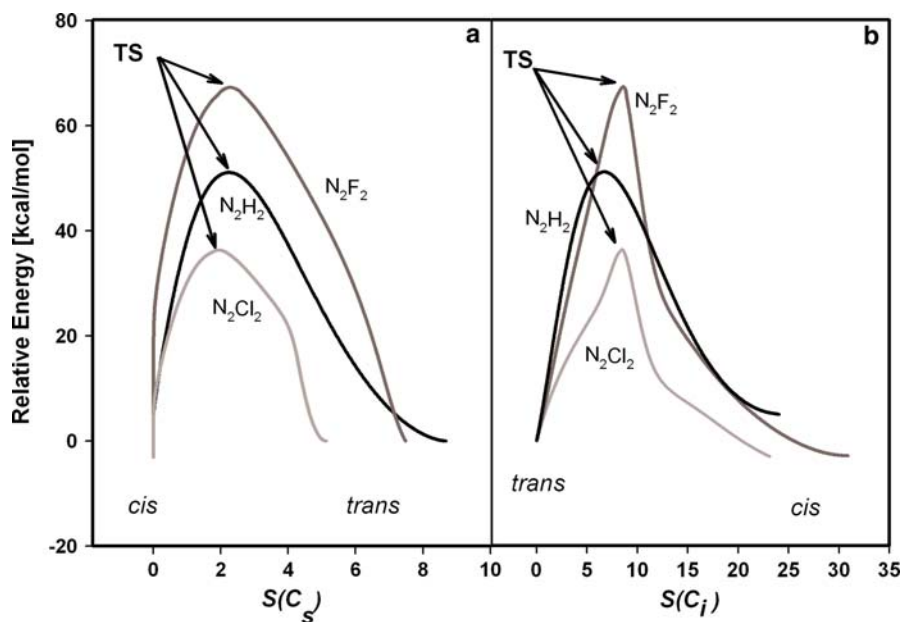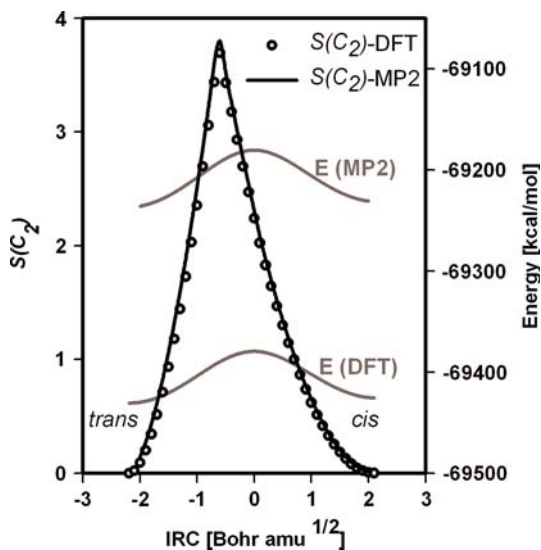
Fig. 8 a Energy profiles of the N_2X_2 *cis* → *trans* isomerization reactions with $S(C_s)$ as the reaction coordinate. **b** Energy profiles of the N_2X_2 *trans* → *cis* isomerization reactions with $S(C_i)$ as the reaction coordinate

ously along the process. Different plots are obtained when the CSM passes through a maximum, as for $S(C_2)$ in our case. Closed loops are obtained, as seen in Fig. 9 (calculated at the B3LYP/CC-PVDZ level; similar plots, not shown here, were obtained at the MP2 level), where the reactant and product are identified by the crossing points with the energy axis ($S(C_2) = 0$). Note that although this is a novel type of a curve,
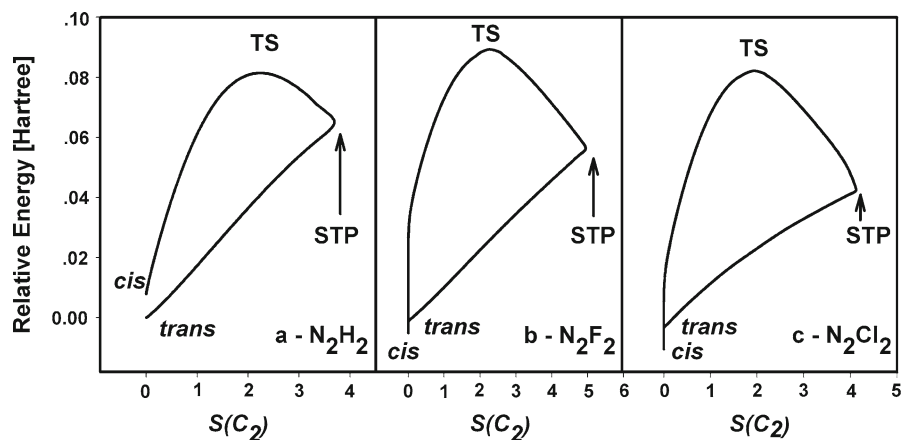
Fig. 9 Energy profiles of the N_2X_2 *cis* → *trans* isomerization reactions with $S(C_2)$ as the reaction coordinate, calculated at the B3LYP/CC-PVDZ level **a** N_2H_2, **b** N_2F_2, **c** N_2Cl_2

the CSM is a "well behaved" coordinate in the sense that it preserves the TS as the maximum point of the plot. The STP points, namely the maximum deviation from C_2 rotational symmetry, characterize the turning point of the loops.

4 Conclusions

In this paper, an analysis of reaction paths in terms of continuous symmetry measures has been presented for the *cis-trans* isomerization reaction of N_2H_2 and for its halogeno derivatives. Symmetry profile plots describe the change in symmetry along the reaction coordinate. This type of plots provides an alternative way to follow reaction paths, using a global structural parameter, additionally to the common use of specific molecular geometry parameters. If the symmetry element chosen characterizes both the reactant and product, a symmetry transition point of a reaction is revealed: a point that marks the switch from a reactant-like molecule to a product-like molecule. For the studied reactions, the deviation from rotational symmetry at the symmetry transition point determines the maximal amount of distortion the reactant undergoes during a reaction in terms of rotational symmetry. If the symmetry element chosen characterizes only one of the reactant or product, then the resulting symmetry profile allows for identification of the reactant and product and can help in the analysis of partial IRC calculations. We showed as well, that CSMs can be useful as alternative reaction coordinates.

In general, the analysis of reaction paths by the CSM offers an alternative way to describe reaction processes. Our results suggest that the approach is hardly affected by the choice of the quantum-mechanical level of theory, as expected from a geometrical parameter. CSMs can be calculated analytically [69] and therefore make the calculations fast and easy to perform. The approach allows for a comparison of reactions in terms of spatial distortions and provides a unique point of view of the structural changes that take place during a reaction.

References

1. K. Fukui, in *Molecular Orbitals in Chemistry, Physics and Biology*, ed. by P.O. Löwdin, B. Pullman (Academic Press, New York, NY, 1964), p 513
2. K. Fukui, *Theory of Orientation and Stereoselection* (Springer, Berlin, 1970)
3. R.B. Woodward, R. Hoffmann, J. Am. Chem. Soc. **87**, 395 (1965)
4. R.B. Woodward, R. Hoffmann, Angewandte Chemie-International Edition **8**, 781 (1969)
5. P.G. Mezey, K. Fukui, S. Arimoto, K. Taylor, Int. J. Quantum Chem. **66**, 99 (1998)
6. P.G. Mezey, Mol. Phys. **96**, 169 (1999)
7. P.G. Mezey, J. Math. Chem. **45**, 544 (2009)
8. L. Leherte, J. Comput. Chem. **27**, 1800 (2006)
9. P.G. Mezey, in *The Reaction Path in Chemistry: Current Approaches and Perspectives*, ed. by D. Heidrich (Kluwer Academic Publishers, Dordrecht, The Netherlands, 1995), p. 11
10. P.G. Mezey, Mol. Phys. **104**, 723 (2006)
11. P.G. Mezey, Mol. Phys. **104**, 2575 (2006)
12. P. Bultinck, X. Girones, R. Carbo-Dorca, Rev. Comput. Chem. **21**(21), 127 (2005)
13. R. Carbo-Dorca, J. Math. Chem. **39**, 551 (2006)
14. X. Girones, R. Carbo-Dorca, QSAR Comb. Sci. **25**, 579 (2006)
15. J.M. Keller, J.C. Bezdek, M. Popescu, N.R. Pal, J.A. Mitchell, J.M. Huband, Int. J. Uncertain. Fuzziness Knowl. Based Syst. **14**, 639 (2006)
16. H. Zabrodsky, S. Peleg, D. Avnir, J. Am. Chem. Soc. **114**, 7843 (1992)
17. H. Zabrodsky, S. Peleg, D. Avnir, J. Am. Chem. Soc. **115**, 8278 (1993)
18. H. Zabrodsky, S. Peleg, D. Avnir, J. Am. Chem. Soc. **115**, 11656 (1993)
19. Y. Salomon, D. Avnir, J. Math. Chem. **25**, 295 (1999)
20. M. Pinsky, D. Casanova, P. Alemany, S. Alvarez, D. Avnir, C. Dryzun, Z. Kizner, A. Sterkin, J. Comput. Chem. **29**, 190 (2008)
21. H. Zabrodsky, D. Avnir, J. Am. Chem. Soc. **117**, 462 (1995)
22. S. Alvarez, P. Alemany, D. Avnir, Chem. Soc. Rev. **34**, 313 (2005)
23. M. Pinsky, D. Avnir, Inorg. Chem. **37**, 5575 (1998)
24. M. Pinsky, K.B. Lipkowitz, D. Avnir, J. Math. Chem. **30**, 109 (2001)
25. S. Alvarez, Dalton Trans. **13**, 2209 (2005)
26. S. Alvarez, P. Alemany, D. Casanova, J. Cirera, M. Llunell, D. Avnir, Coord. Chem. Rev. **249**, 1693 (2005)
27. J. Fornies, A. Martin, L.F. Martin, B. Menjon, H. Zhen, A. Bell, L.F. Rhodes, Organometallics **24**, 3266 (2005)
28. K.M. Ok, P.S. Halasyamani, D. Casanova, M. Llunell, P. Alemany, S. Alvarez, Chem. Mater. **18**, 3176 (2006)
29. A. Ruiz-Martinez, D. Casanova, S. Alvarez, Chem. Eur. J. **14**, 1291 (2008)
30. J. Cirera, E. Ruiz, S. Alvarez, F. Neese, J. Kortus, Chem. Eur. J. **15**, 4078 (2009)
31. D.G. Lonnon, G.E. Ball, I. Taylor, D.C. Craig, S.B. Colbran, Inorg. Chem. **48**, 4863 (2009)
32. G.M. Crippen, Curr. Comput. Aided Drug Des. **4**, 259 (2008)
33. R. Glaser, Chirality **20**, 910 (2008)
34. J. Echeverria, D. Casanova, M. Llunell, P. Alemany, S. Alvarez, Chem. Commun., 2717 (2008)
35. S. Janssens, A. Borgoo, C. Van Alsenoy, P. Geerlings, J. Phys. Chem. A **112**, 10560 (2008)
36. K. Malek, A.P.J. Jansen, C. Li, R.A. Santen, J. Catal. **246**, 127 (2007)
37. M. Llunell, P. Alemany, J.M. Bofill, Theor. Chem. Acc. **121**, 279 (2008)
38. Y. Pinto, P.W. Fowler, D. Mitchell, D. Avnir, J. Phys. Chem. B **102**, 5776 (1998)
39. Y. Pinto, Y. Salomon, D. Avnir, J. Math. Chem. **23**, 13 (1998)
40. P. Alemany, S. Alvarez, D. Avnir, Chem. Eur. J. **9**, 1952 (2003)
41. K. Fukui, J. Phys. Chem. **74**, 4161 (1970)
42. K. Fukui, Acc. Chem. Res. **14**, 363 (1981)

43. B.C. Garrett, M.J. Redmon, R. Steckler, D.G. Truhlar, K.K. Baldridge, D. Bartol, M.W. Schmidt, M.S. Gordon, J. Phys. Chem. **92**, 1476 (1988)
44. C. Gonzalez, H.B. Schlegel, J. Chem. Phys. **90**, 2154 (1989)
45. C. Gonzalez, H.B. Schlegel, J. Chem. Phys. **95**, 5853 (1991)
46. T.J. Lee, J.E. Rice, G.E. Scuseria, H.F. Schaefer, Theor. Chim. Acta **75**, 81 (1989)
47. M.L. McKee, M.E. Squillacote, D.M. Stanbury, J. Phys. Chem. **96**, 3266 (1992)
48. M.L. McKee, D.M. Stanbury, J. Am. Chem. Soc. **114**, 3214 (1992)
49. M.L. McKee, J. Phys. Chem. **97**, 13608 (1993)
50. B.S. Jursic, Int. J. Quantum Chem. **57**, 213 (1996)
51. B.S. Jursic, Chem. Phys. Lett. **261**, 13 (1996)
52. K. Nordhoff, E. Anders, J. Org. Chem. **64**, 7485 (1999)
53. W.A. Sokalski, R.W. Gora, W. Bartkowiak, P. Kobylinski, J. Sworakowski, A. Chyla, J. Leszczynski, J. Chem. Phys. **114**, 5504 (2001)
54. C.H. Lai, M.D. Su, S.Y. Chu, J. Phys. Chem. A **107**, 2700 (2003)
55. X.M. Pu, N.B. Wong, G. Zhou, J.D. Gu, A.M. Tian, Chem. Phys. Lett. **408**, 101 (2005)
56. T. Yamamoto, D. Kaneno, S. Tomoda, J. Org. Chem. **73**, 5429 (2008)
57. D. Bond, J. Phys. Chem. A **113**, 719 (2009)
58. H. Fliegl, A. Kohn, C. Hattig, R. Ahlrichs, J. Am. Chem. Soc. **125**, 9821 (2003)
59. S. Loudwig, H. Bayley, J. Am. Chem. Soc. **128**, 12404 (2006)
60. P. Gorostiza, E.Y. Isacoff, Science **322**, 395 (2008)
61. M. Saljoughian, P.G. Williams, H. Morimoto, D.R. Goodlett, R.B. Vanbreemen, J. Chem. Soc. Chem. Commun. 414 (1993)
62. M.J. Frisch, G.W. Trucks, H.B. Schlegel, G.E. Scuseria, M.A. Robb, J.R. Cheeseman, J.A. Montgomery Jr., T. Vreven, K.N. Kudin, J.C. Burant, J.M. Millam, S.S. Iyengar, J. Tomasi, V. Barone, B. Mennucci, M. Cossi, G. Scalmani, N. Rega, G.A. Petersson, H. Nakatsuji, M. Hada, M. Ehara, K. Toyota, R. Fukuda, J. Hasegawa, M. Ishida, T. Nakajima, Y. Honda, O. Kitao, H. Nakai, M. Klene, X. Li, J.E. Knox, H.P. Hratchian, J.B. Cross, C. Adamo, J. Jaramillo, R. Gomperts, R.E. Stratmann, O. Yazyev, A.J. Austin, R. Cammi, C. Pomelli, J.W. Ochterski, P.Y. Ayala, K. Morokuma, G.A. Voth, P. Salvador, J.J. Dannenberg, V.G. Zakrzewski, S. Dapprich, A.D. Daniels, M.C. Strain, O. Farkas, D.K. Malick, A.D. Rabuck, K. Raghavachari, J.B. Foresman, J.V. Ortiz, Q. Cui, A.G. Baboul, S. Clifford, J. Cioslowski, B.B. Stefanov, G. Liu, A. Liashenko, P. Piskorz, I. Komaromi, R.L. Martin, D.J. Fox, T. Keith, M.A. Al-Laham, C.Y. Peng, A. Nanayakkara, M. Challacombe, P.M.W. Gill, B. Johnson, W. Chen, M.W. Wong, C. Gonzalez, J.A. Pople, Gaussian, Inc., Wallingford, CT 2004.
63. C. Møller, M.S. Plesset, Phys. Rev. **46**, 618 (1934)
64. S.H. Vosko, L. Wilk, M. Nusair, Can. J. Phys. **58**, 1200 (1980)
65. C.T. Lee, W.T. Yang, R.G. Parr, Phys. Rev. B **37**, 785 (1988)
66. A.D. Becke, J. Chem. Phys. **98**, 5648 (1993)
67. P.J. Stephens, F.J. Devlin, C.F. Chabalowski, M.J. Frisch, J. Phys. Chem. **98**, 11623 (1994)
68. T.H. Dunning, J. Chem. Phys. **90**, 1007 (1989)
69. M. Pinsky, C. Dryzun, D. Casanova, P. Alemany, D. Avnir, J. Comput. Chem. **29**, 2712 (2008)